IEEE Photonics Journal
An IEEE Photonics Society Publication

Open Access

Alternative Design of Dammann Grating for Beam Splitting With Adjustable Zero-Order Light Intensity

Volume 11, Number 2, April 2019

Hui Pang
Axiu Cao
Wenjing Liu
Lifang Shi
Qiling Deng

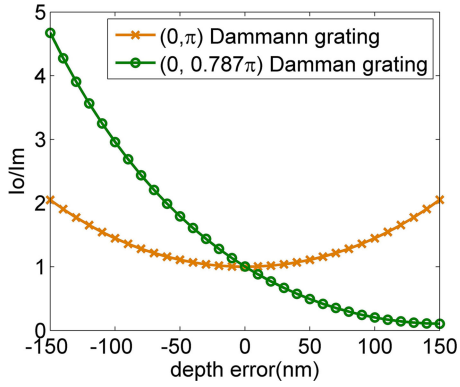

DOI: 10.1109/JPHOT.2019.2899903
1943-0655 © 2019 IEEE

IEEE photonics SOCIETY

IEEE

Alternative Design of Dammann Grating for Beam Splitting With Adjustable Zero-Order Light Intensity

Hui Pang, Axiu Cao, Wenjing Liu, Lifang Shi, and Qiling Deng

Institute of Optics and Electronics, Chinese Academy of Sciences, Chengdu 610209, China

DOI:10.1109/JPHOT.2019.2899903

Manuscript received December 26, 2018; revised February 10, 2019; accepted February 13, 2019. Date of publication February 18, 2019; date of current version March 1, 2019. This work was supported in part by the National Natural Science Foundation of China under Grants 61505214 and 61605211; in part by the Applied Basic Research Programs of Department of Science and Technology of Sichuan Province under Grant 2016JY0175; and in part by the Chinese Academy of Science 'Light of West China' program. Corresponding author: Hui Pang (e-mail: wuli041@126.com).

Abstract: Conventional Dammann grating is a binary-phase (0, π) transmission grating capable of splitting an incoming laser beam into multiple outgoing beams with equal intensity. In this paper, we present an alternative design for Dammann-type beamsplitter with a non π-phase shift value. In the design, the simulated annealing algorithm is taken to optimize the grating structure and phase difference simultaneously. We find that this non 0-π phase grating exhibits interesting properties. When the etching depth is slightly lower than the theoretical depth, the zero-order light intensity is enhanced compared to other diffraction orders. Conversely, when the etching depth is slightly greater than the theoretical depth, the zero-order light intensity is attenuated. This allows us to flexibly adjust the brightness of the zero-order diffractive light. In contrast, the deviation of the etching depth will always result in a brighter zero-order light for the conventional Dammann grating. Simulations and experiments are performed to verify the feasibility of the proposed grating.

Index Terms: Binary optics, diffraction gratings, beam splitting

1. Introduction

An optical array generator is such a device that can divide an incident laser beam into arrays of outgoing beams with specific power distribution [1]. In recent years, it has attracted wide attention due to its great potential in coherent beam combination [2], 3D imaging [3], structured light projectors [4], single-shot ptychography imaging engine [5], THz beam shaping [6] and multi-focus microscopy [7]. Among the wide variety of optical array generators, Dammann grating [8], which is a periodic binary phase (0, π) grating made up of a pattern of alternating areas of different depths, has attracted a considerable amount of interest as its high efficiency and high uniformity [9]–[12]. Till now, Dammann grating has been discussed widely. And the numerical solutions for 1D beam splitting up to 1×32 are already given out [13].

Although these solutions are obtained in order to achieve a uniform intensity distribution, it is easy to achieve a strong zero-order diffracted light by adjusting the etching depth during the processing, which is useful for some applications. Since the relationship between the zero-order intensity and the etching depth is symmetric with respect to the ideal depth and is distributed parabolically

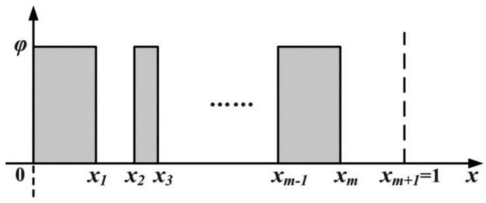

Fig. 1. Typical structure of the coordinate-modulated Dammann grating.

upward. Therefore, as long as there is a deviation between the etching depth and the theoretical depth, the zero-order light intensity is enhanced regardless of the positive or negative depth error [14]–[17]. However, if a weaker zero-order diffracted light is required, redesigning the structure of the grating should be taken to achieve this. So is there any way to easily and flexibly adjust the zero-order light intensity while maintaining the uniformity of other diffraction orders?

Feldman *et al.* have ever proposed a non 0-π binary pure phase grating to improve the diffraction efficiency of the traditional 0-π grating for two-dimensional spot arrays generation [18]. Later in 2017, Bassam *et al.* also took the phase shift value as a free parameter to achieve multicolor beam splitting in multi-focus microscopy [7]. These studies are very innovative and impressive. However, the design methods they proposed are not for the one-dimensional coordinate-modulated Dammann grating, but for the two-dimensional rectangular-aperture-modulated diffraction grating. In addition, the effect of etching depth error on such non 0-π device is also not revealed.

In this paper, we introduce the idea of non 0-π phase difference into the conventional Dammann grating design for beam splitting with adjustable zero-order light intensity. In the design process, the coordinates of the transition points and the phase shift value are taken as variables simultaneously and optimized by the simulated annealing algorithm. Detailed optimization process is presented. And the simulations and experiments are also performed to verify the special property of this modified Dammann grating.

2. Design Method

Fig. 1 is a typical sing-period configuration of coordinate-modulated Dammann grating, which is a two-step pure phase relief structure consisting of a series of grooves with different widths. The grating shape design is to solve the position coordinates of each groove so that the intensity distribution of the desired diffraction order is uniform while the diffraction efficiency is as high as possible. For the conventional Dammann grating, the phase difference φ is not a variable but is directly fixed to π in the design.

According to the basic theory of Fourier optics, the intensity distribution of each diffraction order of this periodic binary phase grating can be obtained by Fourier transform operation of its transmission function, and can be expressed as [19]

$$I_0 = 1 + 4\sin^2(\varphi/2)\left(\sum_i^{m+1}(-1)^i x_i\right)\left(\sum_i^{m}(-1)^i x_i\right), \tag{1}$$

$$I_k = \frac{\sin^2(\varphi/2)}{\pi^2}\frac{1}{k^2}\left\{2\sum_{i=2}^{m+1}\sum_{j=1}^{i-1}(-1)^{i+j}\cos\left[2k\pi\left(x_i - x_j\right)\right] + m + 1\right\}, \tag{2}$$

where I_0 is the zero-order intensity, I_k is the kth order intensity, $\{x_i\}$ are normalized coordinates in one period, and m is the total number of x_i.

Equation (1) gives the mathematical relationship between the zero-order intensity and grating structure and phase difference. According to this formula, we can analyze the influence of phase

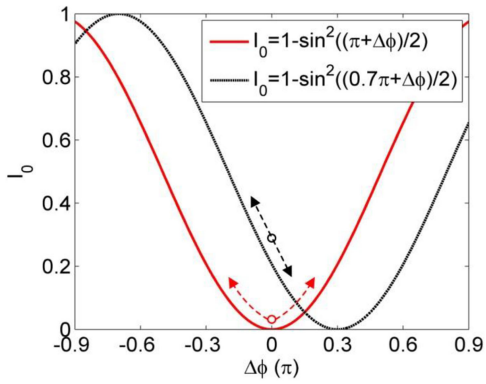

Fig. 2. Effect of phase difference error on the zero-order intensity for the (0, π) and (0, 0.7π) Dammann grating.

difference change on the zero-order light intensity. For the conventional 0-π Dammann grating, Eq. (1) can be rewritten as $I0 = 1 + c \times \sin^2((\pi + \Delta\varphi)/2)$, where c is negative determined by the grating structure and $\Delta\varphi$ represents the phase difference error. Since the value of c does not change the law of the curve, we assume here that $c = -1$. Then the curve $I_0 = 1 - \sin^2((\pi + \Delta\varphi)/2)$ is given in Fig. 2. It can be seen that the intensity curve is symmetrically distributed with respect to $\Delta\varphi = 0$, and I_0 will increase regardless of whether the phase difference error is positive or negative, as indicated by the red arrow in the figure. This is mainly because the sinusoidal function $\sin^2(x)$ is symmetrically distributed with respect to $x = \pi/2$. Therefore, for the conventional Dammann grating, the change in etching depth usually leads to the enhancement of central zero-order diffracted light. So what happens if the theoretical phase difference of the Dammann grating is no longer equal to π? The case where the theoretical phase difference is 0.7π is also presented in Fig. 2 for comparison. We can see that the curve $I_0 = 1 - \sin^2((0.7\pi + \Delta\varphi)/2)$ moves to the right and is no longer symmetrical with respect to $\Delta\varphi = 0$. And the negative phase difference error will cause I_0 enhancement, while the positive phase difference error will cause I_0 weakening, as indicated by the black arrow in the figure. This special property enables us to flexibly adjust the zero-order light intensity to meet some special application needs.

To design the non 0-π Dammann grating, simulated annealing algorithm [20] is adopted, which is an efficient global optimization technique for finding minimum values of a cost function of many independent variables. The detailed process of the design is shown in Fig. 3. Firstly, generate m numbers with three decimal places between 0 and 1 randomly, and arrange them from small to large, representing the coordinates to be optimized. An arbitrary phase difference φ between 0 and π was Chosen and the cost function *cost1* was calculate. It is important to determine the number of coordinate m in each period to provide sufficient free parameters to realize the required beam splitting. Usually, one can refer to the results of 0-π Dammann grating presented in [13] to determine the parameter m. Then change one of the coordinates with $x_i = x_i + 0.001 \times sign(rand - 0.5)$ and recalculate the cost function *cost2*, where *rand* is a random number between 0 and 1, *sign(x)* is the signum function. *Sign(x)* returns 1 if x is greater than zero, 0 if it equals zero and -1 if it is less than zero. If *cost2* is less than *cost1*, the change of x_i is accepted and let *cost1* = *cost2* meanwhile. In addition, if the value of *exp(-Δ/t)* is larger than a random number between 0 and 1, the change still can be accepted, where Δ = *cost2-cost1*, t is the temperature of the annealing process and should be carefully chosen so that the initial probability of acceptance is close to 1. After all the m coordinates have been selected, change the phase difference with $\varphi = \varphi + 0.001 \times sign(rand$-0.5)> and calculate the cost function. The change is accepted with the same condition. Then a single iteration is completed. For each temperature t, this iteration will repeat *num* times. Thereafter the temperature is decreased to $t = t \times 0.9$ to reduce the *exp(-Δ/t)* gradually and then new rounds of

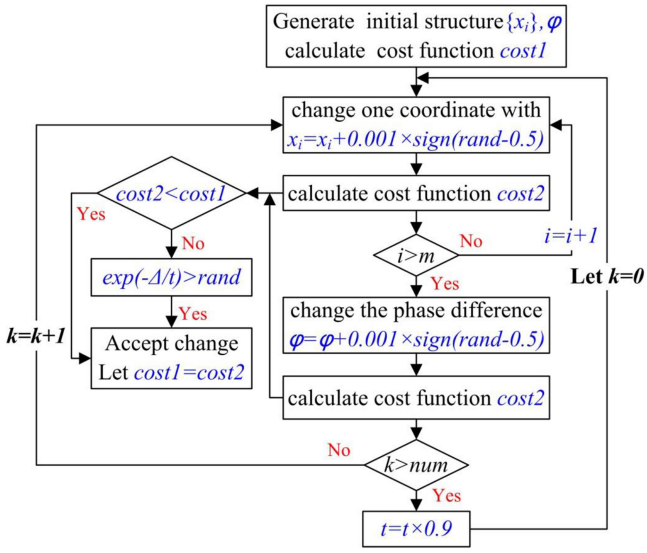

Fig. 3. Flowchart of the simulated annealing algorithm for the non 0-π Dammann grating design.

iterations are performed. Usually, we can stop the iteration process when the cost function is not changed anymore.

The used cost function in the design is a combination of diffraction efficiency and uniformity error [9] and is defined as follows:

$$cost = (\max(I_k) - \min(I_k))^2 + \sum_{k=-n}^{n} (\eta/N - I_k)^2, \tag{3}$$

where η is the desired diffraction efficiency, k is the diffraction order and runs from $-n$ to n with $N = 2 \times n + 1$ for odd number N. When the cost function is minimized, high diffraction efficiency and low uniformity error can be obtained.

3. Simulation

We first consider the problem of a 1×7 array generator. The number of coordinate m is set to 3. One might think that a symmetric grating structure was used in the design because three coordinates yield seven equal intensity orders. In fact, according to Eq. (2), we can clearly see that for the binary phase grating the intensity of I_k is always equal to I_{-k}. Therefore for the required seven equal intensity orders, only four orders: 0, +1, +2, +3 are independent and symmetric grating structure is not necessary in the design. The initial temperature is $t = 1.57$ so that the initial probability of acceptance is 0.99. The iteration number is $num = 300$ for each temperature. The diffraction efficiency η in the cost function is 0.85. The cost function is calculated over the central seven orders (−3,−2,−1, 0, 1, 2, 3). The whole iteration continues about 25000 times and the evolution of the cost function is illustrated in Fig. 4(a). It shows that the changes caused to the increase of the cost function are accepted at the beginning and then rejected when the temperature is lowered. The final value of the cost function is 5.07×10^{-6}. Fig. 4(b) presents the obtained grating structure and its corresponding diffraction efficiency distribution. We can intuitively see that the central seven diffraction orders are very uniform. Calculated diffraction efficiency and uniformity are 84.5% and 99.7%, respectively. The inset is the structure of a single period of the obtained grating. Three coordinates are $x_1 = 0.13$, $x_2 = 0.35$, $x_3 = 0.78$ and the phase difference is 0.787π, not equal to π. By comparison, the efficiency and uniformity obtained by the traditional 0-π Dammann grating are 78.6% and 99.9%, respectively, with coordinates of $x_1 = 0.23191$, $x_2 = 0.42520$, $x_3 = 0.52571$

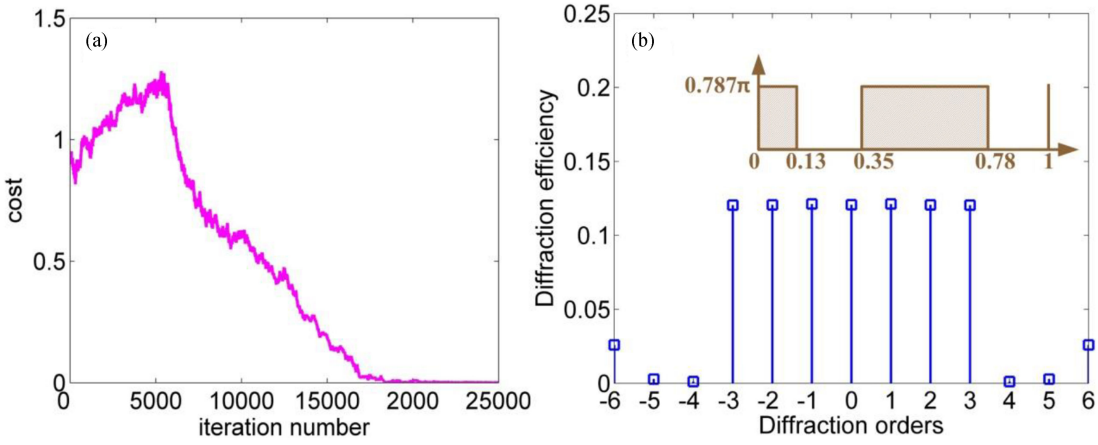

Fig. 4. Design result of the non 0-π Dammann grating (a) cost function curve; (b) grating structure and its diffraction efficiency distribution.

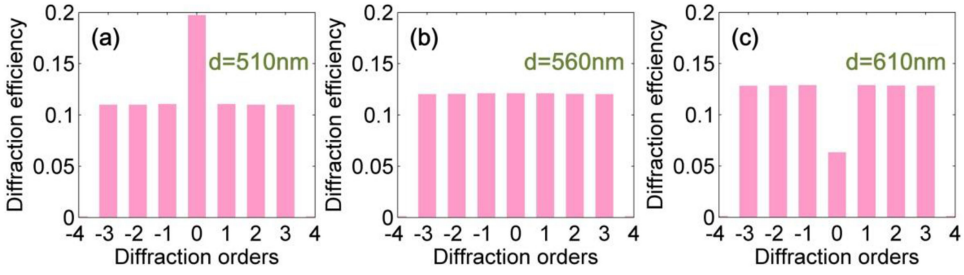

Fig. 5. Diffraction efficiency distribution of the (0, 0.787π) grating with different etching depth (a) d = 510 nm; (b) d = 560 nm; (c) d = 610 nm.

[13]. It concludes that the non 0-π Dammann grating can also achieve the same high diffraction efficiency and uniformity as the conventional 0-π Dammann grating.

Next, we will study the beam splitting performance of these two gratings when the phase difference deviates from the ideal ones. Since the phase difference is related to the etching depth during the processing, the influence of etching depth on the output light intensity distribution is investigated. The physical etching depth d corresponding to the phase delay φ is denoted by:

$$d = \frac{\varphi}{\pi} \times \frac{\lambda}{2\left(n_\lambda - 1\right)} \tag{4}$$

where λ is the wavelength and n_λ is the index of refraction of the substrate at this wavelength. Here, we assume that $\lambda = 650$ nm and n$\lambda = 1.4565$ for fused silica material. Then the accurate etching depth of the (0, 0.787π) Dammann grating is d = 560 nm. By contrast, the ideal etching depth of the traditional (0, π) Dammann grating is d = 712 nm. Fig. 5 shows the beam splitting performance of the (0, 0.787π) Dammann grating at different etching depths. It can be seen intuitively that zero-order diffraction efficiency changes obviously for different depth. When the etching depth is 560 nm, the zero-order efficiency is 12% and is almost the same as other six orders ($\pm$1, $\pm$2, $\pm$3). When the etching depth is decreased to 510 nm, the zero-order efficiency is increased to 20%, while other six orders do not change too much and have an efficiency of about 11%. Conversely, when the etching depth is increased to 610 nm, the diffraction efficiency of the zero order is reduced to 6% and other six orders are maintained at about 13%. This indicates that the zero-order diffracted light of the non 0-π Dammann grating can be flexibly adjusted by change the etching depth while maintaining the uniformity of other diffraction orders. For comparison, the effect of etching depth change on the (0,

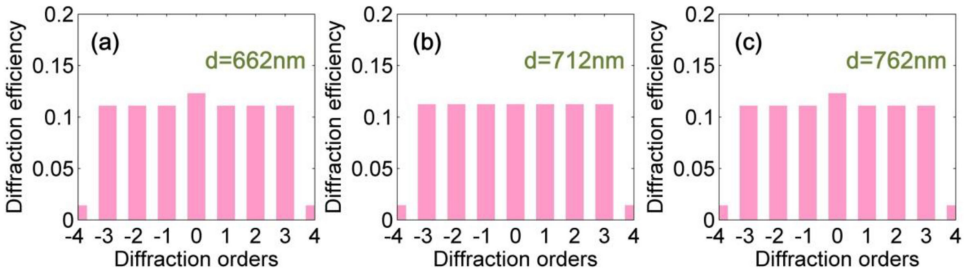

Fig. 6. Diffraction efficiency distribution of the (0, π) grating with different etching depth (a) d = 662 nm; (b) d = 712 nm; (c) d = 762 nm.

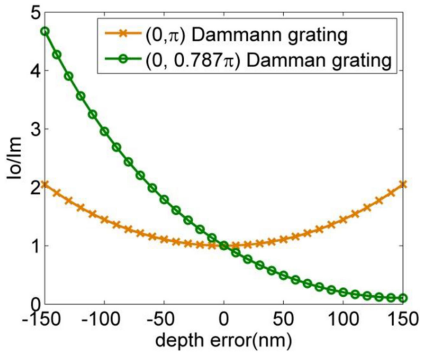

Fig. 7. The ratio of zero-order efficiency to other orders of the two gratings with different depth error.

π) Dammann grating is depicted in Fig. 6. As evident, the zero-order efficiency is higher than other six orders whether the depth is deeper or shallower than the theoretical depth.

It should be noted that although the traditional Dammann grating cannot produce weaker zero-order diffracted light by adjusting the depth, it is less sensitive to depth variations than the non 0-π grating. This is manifested by the fact that when the depth is changed by 50 nm, the zero-order efficiency of the (0, π) grating is only changed by 1%, while the one of the (0, 0.787π) grating is changed by 8%. Therefore, this kind of non 0-π grating requires higher processing requirements. This can be further verified by Fig. 7, which shows the ratio of zero-order diffraction efficiency to the average efficiency of other six orders under different etching depth error.

However, for even-number beam splitters, we find that the optimal phase difference φ is π, which is the same as the traditional Dammann grating. This is because even-number beam splitters require zero-order light intensity to be zero and the zero-order light intensity is equal to the interference of the two areas of the grating. Only when the phase difference between the two areas is π, the destructive interference is complete and the zero order is missing.

4. Experiments and Discussion

To verify the simulation results, the improved Dammann grating for 1 $\times$ 7 beam splitting for 650 nm laser with fan-out angle of 2.23 degree was designed and fabricated. According to the grating diffraction equation, the grating period is 3 $*$ 650 nm/sin(22.7/2) $=$ 100 um. Thereafter detailed grating structure can be fixed according to the coordinates of the transition points shown in Fig. 4. The calculated minimum feature size of the grating is 0.13 $*$ 100 um $=$ 13 um, which allows us to use the conventional photolithography and etching techniques. The fabrication process mainly includes photoresist coating, exposure, development and etching. Silica with refractive index of 1.4565 at 650 nm wavelength was chosen as the substrate. Then the accurate etching depth corresponding to

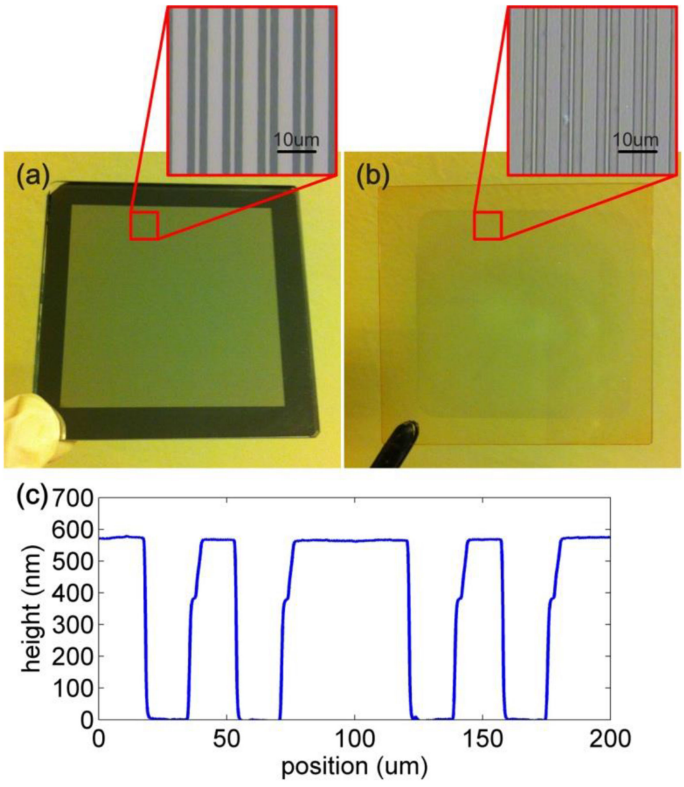

Fig. 8. (a) The mask. (b) The fabricated grating, and its surface profile. (c) measured with step profilometer.

the phase difference of 0.787π is 560 nm. The AZ1500 (AZ Electronic Materials, Somerville, USA) was used as the photoresist, which was spin-coated on the substrate at a speed of 5000 rpm for 30 s. Key parameters such as prebake temperature, prebake period, and thickness of photoresist were 90 °C, 10 min, and 3 um, respectively. The illumination light source was an Hg lamp with a central wavelength of 365 nm, which was the ultraviolet part of the spectrum (UV). The total exposure time was 10 s at an exposure power density of 3 mW cm^2. Then, the photoresist was developed in a solution of AZ300MIF for 30 s, followed by 120 min post-exposure bake at 120 °C. Finally, reactive ion etching machine was used to transfer the structure into the substrate. The etching gases were SF_6 and CHF_3 in the proportion of 1:40 and the etching time was about 14 min for a depth of 560 nm.

Fig. 8(a) is the mask for exposure, and the inset is a micrograph of the internal structure. The black equal-width slits are light transmissive areas with a width of 22 um. The white portions are opaque areas with widths of 13 um and 43 um. The etching rate corresponding to different slit widths will vary during reactive ion etching. Therefore, two identical regions having a slit width of 22 um are selected as the etched regions to ensure that the final grating is a two-step structure. The fabricated grating is shown in Fig. 8(b), and it can be seen that it preserves the characteristics of the mask very well. The step profilometer (Stylus Profiler System, Dektak XT, Bruker, Karlsruhe, Germany) is used to measure the surface profile of the grating and the result is presented in Fig. 8(c). The achieved average etching depth is about 565 nm, which deviates from the desired value 560 nm slightly. In addition, by adjusting the etching time to 12 minutes and 16 minutes, we also obtained two other gratings with depth of 430 nm and 680 nm.

Then optical experiments are performed to test the performance of these three fabricated gratings. The schematic diagram of the experimental setup is given in Fig. 9(a). The fabricated grating is

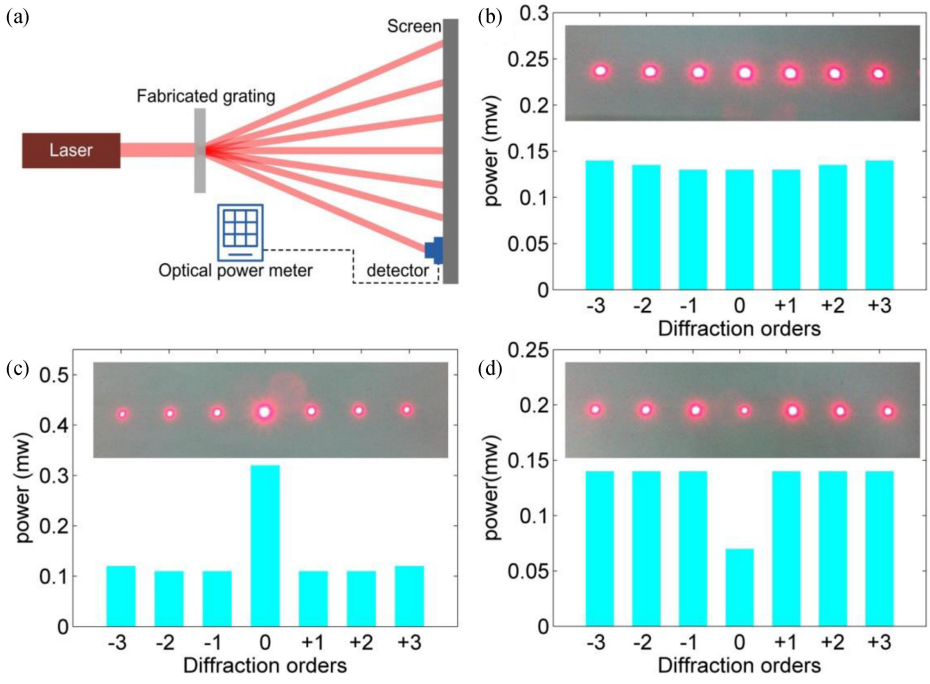

Fig. 9. (a) The setup for the power measurement. Obtained power distribution of the three fabricated gratings with depth of (b) 565 nm, (c) 430 nm, (d) 680 nm.

placed in parallel with the observation screen. The collimated laser of 650 nm wavelength is vertically incident on the grating, and multiple diffraction orders of light are generated on the screen. The optical power meter (PD300-UV-ROHS, Ophir, Israel) is used to measure the light energy distribution of the diffraction orders. Fig. 9(b) shows the power distribution of the grating with etching depth of 565 nm. The inset is the corresponding photo of diffraction pattern taken by the camera. The optical powers of the -3, -2, -1, 0, $+1$, $+2$ and $+3$ orders are 0.14 mW, 0.135 mW, 0.13 mW, 0.13 mW, 0.13 mW, 0.135 mW and 0.14 mW, respectively. The calculated uniformity is $[1 - (0.14 - 0.13)/(0.14 + 0.13)] \times 100\% = 96.3\%$, which is slightly lower than the theoretical result 99.7%. This deviation is mainly caused by the imperfect grating structure, which can be further improved by process optimization. Fig. 9(c) shows the power distribution of the grating with etching depth of 430 nm. The powers of the central seven diffraction orders are 0.12 mW, 0.11 mW, 0.11 mW, 0.32 mW, 0.11 mW, 0.11 mW and 0.12 mW, respectively. It can be seen that the zero-order power is significantly enhanced, while the energy of the other six diffraction orders are weakened. Fig. 9(d) shows the power distribution of the grating with etching depth of 680 nm. The corresponding measured powers of the seven diffraction orders are 0.14 mW, 0.14 mW, 0.14 mW, 0.07 mW, 0.14 mW, 0.14 mW and 0.14 mW, respectively. We can clearly see that the zero-order diffracted light is effectively weakened, and the power distribution of the other six orders is still relatively uniform. The experimental results are consistent with the simulation results, which verify the zero-order adjustable function of the proposed non 0-π Dammann grating.

5. Conclusion

In summary, an alternative design for Dammann-type beamsplitter with non 0-π phase shift value is proposed. In comparison with the traditional 0-π Dammann grating, the zero-order diffracted light intensity of the proposed grating can be adjusted flexibly. When the etching depth is slightly lower than the theoretical depth, the zero-order light intensity is enhanced. Conversely, when the etching

depth is slightly greater than theoretical depth, the zero-order light intensity is attenuated. It can be expected that the proposed grating would be applied in laser beam splitting.

References

[1] S. J. Ge *et al.*, "Optical array generator based on blue phase liquid crystal Dammann grating," *Opt. Exp.*, vol. 6, no. 4, pp. 1087–1092, Apr. 2016.
[2] S. B. Li and Y. C. Lu, "Improvement of the image quality of random phase-free holography using an iterative method," *Opt. Commun.*, vol. 407, pp. 321–326, Feb. 2018.
[3] S. B. Wei, C. H. Zhou, S. Q. Wang, K. Liu, X. Fan, and J. Y. Ma, "Colorful 3-D imaging using an infrared Dammann grating," *IEEE Trans. Ind. Informat.*, vol. 12, no. 4, pp. 1641–1648, Aug. 2016.
[4] O. Barlev and M. A. Golub, "Multifunctional binary diffractive optical elements for structured light projectors," *Opt. Exp.*, vol. 26, no. 16, pp. 21092–21107, Aug. 2018.
[5] X. He, X. C. Pan, C. Liu, and J. Q. Zhu, "Single-shot phase retrieval based on beam splitting," *Appl. Opt.*, vol. 57, no. 17, pp. 4832–4838, Jun. 2018.
[6] K. Liebert *et al.*, "THz beam shaper realizing fan-out patterns," *J. Infrared Millim. THz Waves*, vol. 38, pp. 1019–1030, May 2017.
[7] B. Hajj, L. Oudjedi, J. B. Fiche, M. Dahan, and M. Nollmann, "Highly efficient multicolor multifocus microscopy by optimal design of diffraction binary gratings" *Sci. Rep.*, vol. 7, Jul. 2017, Art. no. 5284.
[8] H. Dammann and K. Gortler, "High-efficiency in-line multiple imaging by means of multiple phase holograms," *Opt. Commun.*, vol. 3, no. 5, pp. 312–315, Jul. 1971.
[9] J. Jahns, M. M. Downs, M. E. Prise, N. Streibl, and S. J. Walker, "Dammann gratings for laser beam shaping," *Opt. Eng.*, vol. 28, no. 12, pp. 1267–1275, Dec. 1989.
[10] Y. Y. Ma, C. C. Ye, J. Ke, J. Y. Zhang, J. Q. Zhu, and Z. Q. Ling, "Array illumination of a Fresnel–Dammann zone plate," *Appl. Opt.*, vol. 55, no. 26, pp. 7218–7221, Sep. 2016.
[11] H. A. Hajjar, B. Fracasso, and K. Heggarty, "Uniform free-space cell shaping using diffractive-type beam diffusers for optical wireless links," *Opt. Lett.*, vol. 39, no. 24, pp. 6871–6874, Dec. 2014.
[12] J. N. Mait, "Design of binary-phase and multiphase Fourier gratings for array generation," *J. Opt. Soc. Amer. A*, vol. 7, no. 8, pp. 1514–1528, Aug. 1990.
[13] C. H. Zhou and L. R. Liu, "Numerical study of Dammann array illuminators," *Appl. Opt.*, vol. 34, no. 26, pp. 5961–5969, Sep. 1996.
[14] S. X. Li, G. Yu, C. Y. Zheng, and Q. F. Tan, "Quasi-Dammann grating with proportional intensity array spots," *Opt. Lett.*, vol. 33, no. 18, pp. 2023–2025, Sep. 2008.
[15] Q. K. Li *et al.*, "Sapphire-based Dammann gratings for UV beam splitting," *IEEE Photon. J.*, vol. 8 no. 6, Dec. 2016, Art. no. 2500208.
[16] X. Q. Wang *et al.*, "Electrically/optically tunable photo-aligned hybrid nematic liquid crystal Dammann grating," *Opt. Lett.*, vol. 41, no. 24, pp. 5668–5671, Dec. 2016.
[17] D. C. O. Shea, "Reduction of the zero-order intensity in binary Dammann gratings," *Appl. Opt.*, vol. 34, no. 28, pp. 6533–6537, Oct. 1995.
[18] M. R. Feldman and C. C. Guest, "Iterative encoding of high-efficiency holograms for generation of spot arrays," *Opt. Lett.*, vol. 14, no. 10, pp. 2023–2025, May 1989.
[19] U. Killat, G. Rabe, and W. Rave, "Binary phase gratings for star couples with high splitting ratio," *Fiber Integr. Opt.*, vol. 4, no. 2, pp. 159–167, Feb. 1982.
[20] S. Kirkpatrick, C. D. Gelatt, and M. P. Vecchi, "Optimization by simulated annealing," *Science.*, vol. 220, no. 4598, pp. 671–680, May 1983.